

The Evolution of Dropsonde-derived Vorticity in Developing and Non-developing Tropical Convective Systems

CHARLES N. HELMS * AND ROBERT E. HART

Florida State University, Tallahassee, Florida

1. Introduction

The process by which tropical cyclones evolve from loosely organized convective clusters into well organized systems is still poorly understood. The primary challenge when studying tropical cyclogenesis is the remote, data-sparse locations in which it occurs. Observation-based studies of the processes by which genesis occurs can be divided into two main groups based on how this challenge is handled. The first of these groups uses composites of data gathered from a large number of individual cases to construct an image of the ‘typical’ structure of a tropical system (e.g. McBride and Zehr 1981). The latter group includes studies examining a small number of individual systems in great detail in order to identify key features which may otherwise be removed in a composited mean (e.g. Simpson et al. 1997).

The present study falls into the second of the above categories and aims to perform a detailed analysis of the three-dimensional structural evolution of vorticity with the goal of highlighting differences in developing and non-developing tropical convective systems. For brevity, only two systems are analyzed below. The data used is briefly covered in the next section followed by an overview of the methodology used for the analyses. The results are presented in section 4 and section 5 provides some conclusions based on these results.

2. Data

The analysis presented here uses GPS dropsonde measurements from two field campaigns: the Pre-depression Investigation of Cloud Systems in the Tropics (PREDICT,

* *Corresponding author address:* Charles N. Helms, Dept. of Earth, Ocean, and Atmospheric Sciences, Florida State University, Tallahassee, Florida 32306-4520
E-mail: chip.helms@gmail.com

Montgomery et al. 2011) experiment and the Genesis and Rapid Intensification Processes (GRIP) experiment. Data support for both experiments is provided by NCAR/EOL under sponsorship of the National Science Foundation. It is important to note that the dropsonde observations from these field experiments are rarely taken within deep convection and, as a result, the calculations are assumed to represent a combination of the background fields and the impacts of the convection on the environment.

Since the observation times are not simultaneous, a time correction is applied by advecting each observation to a common time by its corresponding observed wind. While the flow is primarily zonal in pre-genesis disturbances, in instances where the meridional component of the wind has a magnitude approaching or exceeding that of the zonal wind, the magnitudes are sufficiently low such that any error due to acceleration is minimal.

3. Methodology

Spatial derivatives (e.g. vorticity) are calculated by applying Green’s theorem. For a region bounded by the circuit C and having area A ,

$$\frac{\partial Q}{\partial x} - \frac{\partial P}{\partial y} = \frac{\oint_C P dx + Q dy}{A} \approx \frac{\sum(P\Delta x + Q\Delta y)}{A}, \quad (1)$$

where Q and P are arbitrary variables and Δx and Δy are the zonal and meridional components of the edge lengths, respectively. By assigning the proper variables and signs to Q and P in Eq. (1) any spatial derivative can be calculated. In the case of vorticity, the substitution is relatively simple and results in

$$\frac{\partial v}{\partial x} - \frac{\partial u}{\partial y} \approx \frac{\sum(u\Delta x + v\Delta y)}{A}, \quad (2)$$

where u and v are the zonal and meridional wind components, respectively. For the present study, irregular poly-

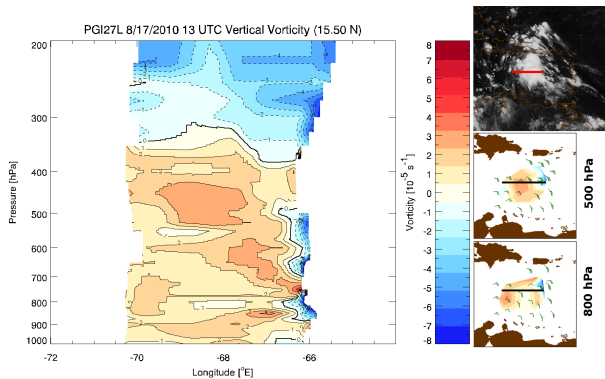


FIG. 1. Cross-section of vertical relative vorticity for PGI27L along 15.5°N on Aug. 17, 2010 at 13 UTC. The vertical resolution of the cross-section is 25 hPa and contours are plotted in intervals of 10^{-5} s^{-1} . Inset on the right, in order from top to bottom, are the geostationary infrared satellite representation, the 500 hPa vorticity plot, and the 800 hPa vorticity plot. The horizontal red and black bars on the inset frames represent the location of the cross-section data.

gons are used to define the regions on which Green’s theorem is applied. The process for constructing these polygons is explained and evaluated in detail by Helms and Hart (2012, P2.7). It is also of importance to note that Green’s theorem results in smaller magnitudes of the extrema.

4. Results

a. PGI27L

PGI27L was a non-developing system associated with an easterly wave which moved off of Africa on August 9, 2010. It moved into the Caribbean Sea on August 16 and into the Gulf of Mexico on August 20. The PREDICT campaign flew two missions into PGI27L on August 17 and 18 while the system was over the central Caribbean Sea.

The first mission took place near the peak of the second convective maximum, as identified by periods of large MCS-like features. The convection associated with this maximum occurred further north along the wave axis than during the previous convective maximum. As the new convection would not have access to the previously generated vorticity, this shift may explain the relatively smaller vorticity magnitudes apparent in Fig. 1 in comparison to the values shown in Fig. 2 from the following day. Additionally, strong shear and a mid-level region of very dry air (below 30% relative humidity, not shown) located to the northeast and the west may be inhibiting convective organization and, as a result, diminishing vorticity production. A region of strong divergence (Fig. 3), maximized near the surface, is located within the deep convection and likely indicates the presence of a strong downdraft.

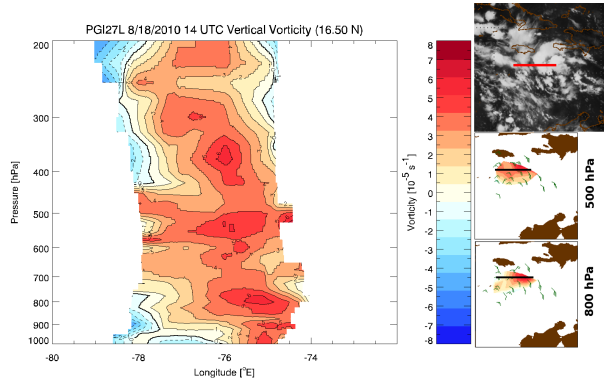


FIG. 2. Same as Fig. 1 except on Aug. 18, 2010 at 14 UTC along 16.5°N.

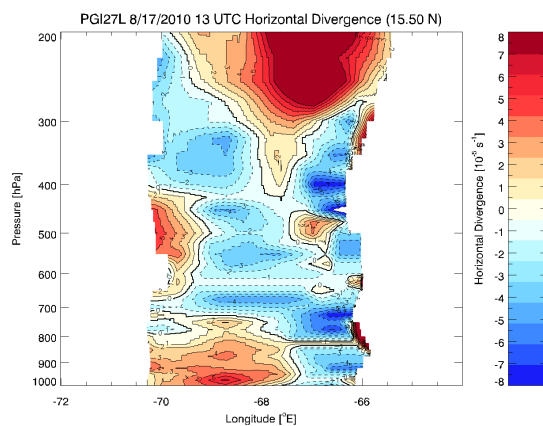


FIG. 3. Cross-section of horizontal divergence corresponding to Fig. 1. The vertical resolution is 25 hPa and contours are plotted in intervals of 10^{-5} s^{-1} .

During the convective maximum on August 18 the cyclonic vorticity is seen to extend throughout the depth of the troposphere (Fig. 2). The dry air present at mid-levels the previous day is observed on the west side of the system and is assumed to still be present northeast of the observation domain. Although relative humidity values in the dry air regions have risen from the previous day, values approaching 30% are still present at the mid-levels. The strong surface divergence associated with the downdraft is no longer located beneath the deepest convection and has been replaced by strong surface convergence. This transition may suggest the formation of the downdraft-free convection implicated in the genesis process by Bister and Emanuel (1997).

b. PGI44L

The initial PGI44L disturbance formed on Sept. 8, 2010 in association with the interaction of a trough over South

America and an easterly wave (Stewart 2011). The system was labeled as a tropical depression on Sept. 14 at 12 UTC and became TS Karl on Sept. 14 at 18 UTC. In total, 11 missions were flown into the system from Sept. 10 through Sept. 17 by both PREDICT and GRIP.

As was the case with PGI27L, the first mission into PGI44L occurred near the peak of the convective maximum. By this time, the low-level circulation was already very well defined below 700 hPa (Fig. 4). The cross-section also suggests the presence of a mid-level region of cyclonic vorticity between 400 hPa and 600 hPa on the western edge of the observation domain. Closer examination of the satellite representation shows that the cross-section (red bar, top right corner of Fig. 4), as well as the observation domain, are situated east of a region of deep convection which could be associated with a mid-level vorticity maximum. Additionally, the strong mid-level vorticity feature seen the next day (Fig. 5) is unlikely to have formed without the presence of a pre-existing feature.

Co-located with the low-level vorticity maximum on Sept. 10 is an area of strong low level convergence beneath a layer of strong divergence (Fig. 7). Based on this, one possible explanation for the presence of the low level vorticity maximum is the concentration and stretching of background vorticity by rising motion, a process featured prominently in a number of genesis theories (e.g. Montgomery et al. 2006). It is interesting to note that this couplet is seen to be reversed during a mission into PGI44L later the same day (not shown). On Sept. 11, the atmosphere below 900 hPa has weak convergence below a layer of weak divergence (Fig. 8). The corresponding low-level vorticity maximum is contained primarily below 800 hPa, suggesting that the process of concentrating and stretching background vorticity may again be at work in the lower atmosphere.

Although the low-level and mid-level vorticity maxima have become vertically aligned by Sept. 13 (Fig. 6), the observed wind field does not indicate a closed circulation. One possibility is that a closed circulation is located to the south of the observation domain, placing it just outside of the deep convection. Alternatively, the tropical cyclone report (Stewart 2011) suggests a temporary interruption in the genesis process occurred, briefly resulting in the loss of a closed circulation. As there is no signature of a circulation evident in the cloud patterns, it is likely that the circulation has weakened momentarily. Despite this weakening, the system rapidly spins up and is named a tropical storm the next day.

5. Conclusions

While an examination of only one developing case and one non-developing case prevents making general conclusions regarding the differences between developing and non-

developing tropical convective systems, it is worthwhile to highlight a number of differences and similarities between the two cases presented above. First, it should be noted that both systems are vertically aligned at some point during their evolution. The primary difference between the two systems while they are vertically aligned is seen in the magnitude of the vorticity, with the developing system having larger values of relative vorticity.

In the non-developing system, evidence of a strong downdraft is seen located beneath the deep convection during the first missions but is not seen during the next day. With the exception of a single mission, the developing case does not display this evidence. The presence of a downdraft beneath the deep convection inhibits the strength of the nearby updraft. With a reduction in updraft velocities there should also be a corresponding reduction in surface convergence, by mass continuity arguments. As a result, the downdraft would have a net effect of reducing vorticity spin-up by inhibiting the concentration and stretching of background vorticity. It seems that at some point both systems may have developed downdraft-free convection. If this is the case, then it is possible that the non-developing system may have failed to intensify due to the presence of mid-level dry air creating a favorable environment for downdraft formation associated with evaporative cooling. Land interaction may also have played a role as the non-developing system passed closer to the Greater Antilles and reached the Yucatan peninsula earlier in its evolution than did the developing system.

As was previously noted, these conclusions are solely based on two cases and, as a result, it is difficult to generalize to tropical cyclogenesis as a whole. Additional case analyses are planned to help reduce this issue and these conclusions are intended to serve as a starting point for gaining a better understanding of the bifurcation between developing and non-developing systems.

Acknowledgments.

The authors would like to thank Bob Dattore for his efforts in providing data from a number of field experiments which have yet to be incorporated into the analysis. Additionally, discussions with Jack Beven and Chris Davis greatly aided the analysis process. This work is funded through the NASA Genesis and Rapid Intensification Processes (GRIP) Grant #NNX09AC43G.

REFERENCES

- Bister, M., and K. A. Emanuel, 1997: The genesis of Hurricane Guillermo: TEXMEX analyses and a modeling study. *Mon. Wea. Rev.*, **125**, 2662–2682.
- Helms, C. N., and R. E. Hart, 2012: A polygon-based line

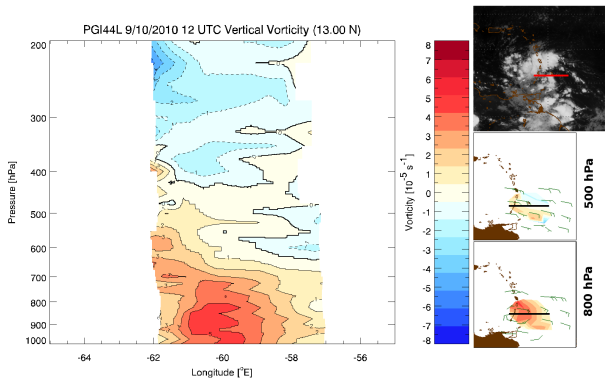


FIG. 4. Same as Fig. 1 except for PGI44L on Sept. 10, 2010 at 12 UTC along 13°N.

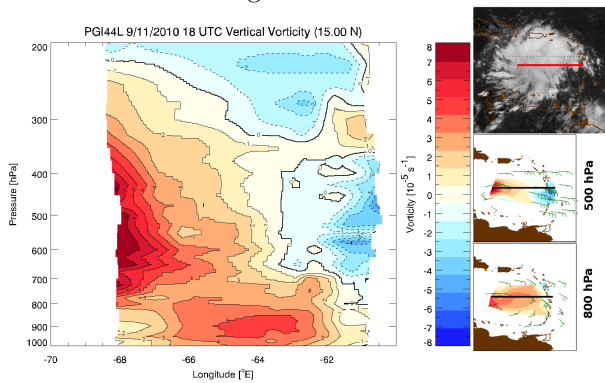


FIG. 5. Same as Fig. 1 except for PGI44L on Sept. 11, 2010 at 18 UTC along 15°N.

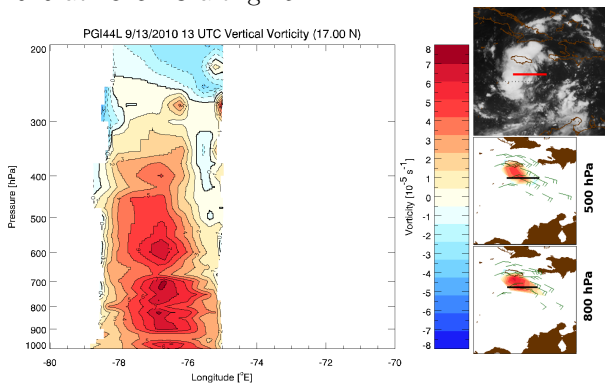


FIG. 6. Same as Fig. 1 except for PGI44L on Sept. 13, 2010 at 13 UTC along 17°N.

integral method for calculating vorticity, divergence, and deformation from non-uniform observations. *Extended Abstracts, 30th Conf. on Hurricanes and Tropical Meteorology*, Ponte Vedra, Florida, Amer. Meteor. Soc.

McBride, J. L., and R. Zehr, 1981: Observational analysis of tropical cyclone formation. Part II: Comparison of non-developing versus developing systems. *J. Atmos.*

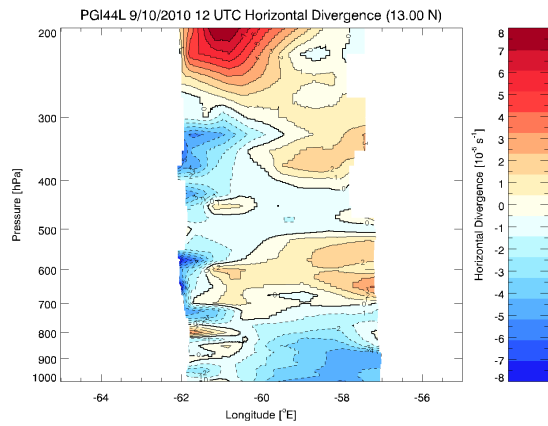


FIG. 7. As in Fig. 3 except corresponding to Fig. 4.

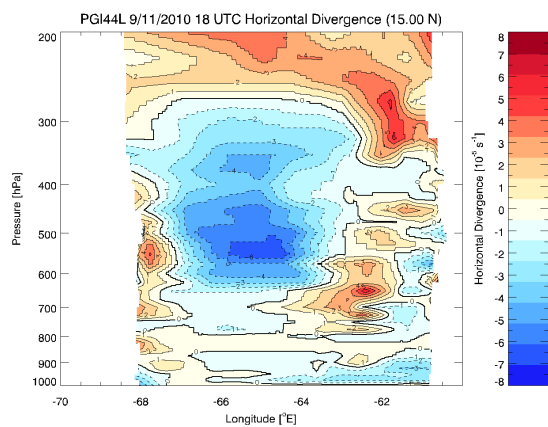


FIG. 8. As in Fig. 3 except corresponding to Fig. 5.

Sci., **38**, 1132–1151.

Montgomery, M. T., M. E. Nicholls, T. A. Cram, and A. B. Saunders, 2006: A vortical hot tower route to tropical cyclogenesis. *J. Atmos. Sci.*, **63**, 355–386.

Montgomery, M. T., and Coauthors, 2011: The pre-depression investigation of cloud systems in the tropics (PREDICT): Scientific basis, new analysis tools and some first results. *Bull. Amer. Meteor. Soc.*, **93**, 153–172.

Simpson, J., E. A. Ritchie, G. J. Holland, J. Halverson, and S. Stewart, 1997: Mesoscale interactions in tropical cyclone genesis. *Mon. Wea. Rev.*, **125**, 2643–2661.

Stewart, S. R., 2011: Tropical cyclone report, Hurricane Karl, 14–18 September 2010. National Hurricane Center, 17 pp. [Available online at www.nhc.noaa.gov/pdf/TCR-AL132010-Karl.pdf.]